Mechatronics 24 (2014) 519–532

Contents lists available at ScienceDirect

Mechatronics

journal homepage: www.elsevier.com/locate/mechatronics

Double-level ball-riding robot balancing: From system design, modeling, controller synthesis, to performance evaluation

Kanjanapan Sukvichai *, Manukid Parnichkun

Mechantronics, Asian Institute of Technology, P.O. Box 4, Klong Luang, Pathumthani 12120, Thailand

ARTICLE INFO

Article history:
Received 9 September 2013
Accepted 10 June 2014
Available online 14 July 2014

Keywords:
Ball-riding robot
Non-linear system
Sensor fusion
Linear Quadratic Regulator plus Integral

ABSTRACT

In this research, a new robot, double-level ball-riding robot, is introduced. The robot consists of an upper ball-riding subsystem and a lower ball-riding subsystem. The robot's dynamics model can be considered separately in two identical planes. Euler–Lagrange equation of motion is applied in order to obtain the dynamics model. Motors are included in the robot's model. The model is then linearized. The robot's parameters are identified. The robot's prototype is manufactured and assembled. Linear Quadratic Regulator with Integral (LQR + I) controller is proposed and applied in order to balance both levels of the robot. The complementary and orientation transformation are used to fuse sensors in order to obtain robot leaning angles. Balancing performance of the developed double-level ball-riding robot is evaluated by simulations and experiments. The results show efficient control performance of LQR + I controller.

1. Introduction

Balancing of unstable robot is one of the most challenge topics for researchers in the field of dynamics control. Ball-riding robot or BallBot is an interesting topic from both mechanism and a controller design aspects since the robot is usually a non-linear unstable system. It requires appropriate controller to make the robot become stable. The pioneer work of BallBot was introduced by Lauwers et al. [1] from Carnegie Mellon University (CMU) in 2005. This BallBot used concept of inverted mouse driving mechanism and it was controlled by LQR + PI algorithm. In 2008, Peng et al. [2] and Ching-Wen and Ching-Chih [3] introduced ball-riding robots which changed the driving wheels from regular solid fixed wheels, which were used in CMU BallBot, to omni-directional wheels. Kumagai and Ochiai [4] demonstrated cooperative BallBots for the first time. These BallBots could perform more complicated tasks such as object carrying using human-robot or multi-robot cooperation. Fankhauser and Gwerder [5] introduced a service BallBot which could move in high speed. Lotfiani et al. [6] focused on a trajectory tracking motion of a single level robot. Although, these BallBots could be balanced successfully, all the BallBots still have only single level.

Double-level ball-riding robot is a system which contains two cooperative Ballbots. An upper level Ballbot rides on top of a lower level Ballbot. There is a limitation when constructing a tall single-level Ballbot which has large moment of inertia since it requires large actuators in order to balance the Ballbot.

Multi-level ball-riding robot can solve this problem. By placing a short Ballbot on top of another short Ballbot, the robot will be taller. The number of levels depends on the required height. Since the short Ballbot has small moment of inertia, it requires only small actuators.

Furthermore, a multi-level ball-riding robot is more flexible than a single-level ball-riding robot. By controlling the motion of each level cooperatively, a very stable system can be achieved. It can even perform the motion like robot manipulator. This concept can be extended to a building which can resist earthquake. Last but not least important in dynamic control course, it is an excellent platform to test control performance of different control algorithms. In this research a double-level ball-riding robot is introduced. The mechanism is designed and developed. Both levels of the robot are then controlled by using an optimal controller.

2. Mechanic design

Each level of the robot is designed by using inverted mouse mechanism. The mathematical model can be derived easily since the sagittal and coronal planes of the robot are decoupled. Each level of the robot is driven by four driving wheels attached to 100 W DC motors through belt and pulley transmission. Driving wheels are placed in perpendicular to the ball surface at a distance from the ball center. The inverted mouse mechanism of each level of the robot is shown in Fig. 1. In the original design, the robot

* Corresponding author. Tel.: +66 2 524 6054; fax: +66 2 524 6432.
E-mail address: st111444@ait.ac.th (K. Sukvichai).

http://dx.doi.org/10.1016/j.mechatronics.2014.06.003
0957-4158/

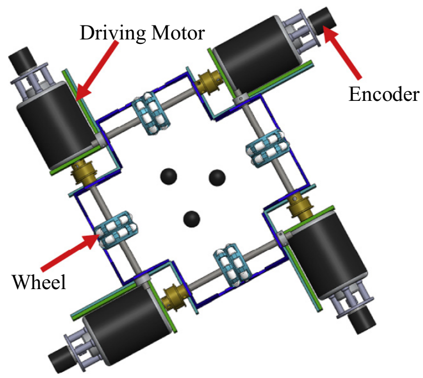

Fig. 1. Driving mechanism of double-level ball-riding robot.

wheels are made from nylon tubes. Even though the nylon-tube wheels can be used to drive the robot, however there is a problem of large friction between the ridden ball and the nylon-tube wheels when the ridden ball moves in perpendicular to the wheel rotating axis. Furthermore, since the ridden ball always deforms caused by the robot weight, the ball cannot be considered as a solid spherical ball. The ball deformation results in change of the contact type between the ball and wheels from point contacts to area contacts.

The increasing friction creates nonlinear behavior. This effect is more severe when the upper-level subsystem is placed on top of the lower-level subsystem. By introducing omni-directional wheels, these problems are solved. Each omni-directional wheel has two degree of freedoms. Wheel rollers help reduce friction between the ball and the wheel. The friction then becomes small. Omni-directional wheels are selected as robot driving wheels. Two identical ball-riding subsystems are used for both lower and upper levels.

However the ridden ball of the upper subsystem is attached to the chassis of the lower subsystem. The double-level ball-riding robot is shown in Fig. 2.

3. Robot Dynamics model

3.1. Mechanical model

Dynamics model of the double-level ball-riding robot in x–z and y–z planes are identical because of the symmetry of the robot's structure. The lower and upper balls have the same radius. The dynamics model of each plane is derived from the projection image as shown in Fig. 3.

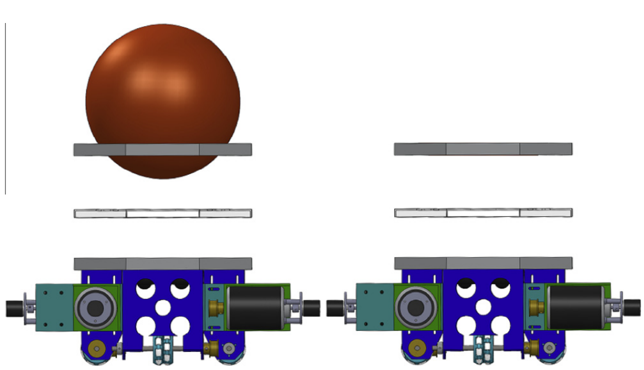

Fig. 2. Lower (left) and upper (right) subsystems.

The Euler–Lagrange equation of motion is used to derive dynamics model of the double-level ball-riding robot. Friction in the system is assumed small and negligible. The dynamics equation is obtained using Eq. (1).

$$\frac{d}{dt}\left(\frac{\partial L}{\partial \dot{q}}\right) - \frac{\partial L}{\partial q} = \bar{f}_{NP} \tag{1}$$

Lagrangian, L, is the difference between total kinetic energy, K, and total potential energy, P, of the robot and is expressed as $L = \sum K - \sum P$. The value of L is shown in Appendix A. By solving Eq. (1), the dynamics equations of the robot are obtained as shown in Eqs. (2)–(4).

$$\begin{aligned}
\frac{d}{dt}\left(\frac{\partial L}{\partial \dot{\phi}}\right) - \frac{\partial L}{\partial \phi} = & - m_u r_b k_2 \mathrm{Sin}(\beta+\theta)\dot{\beta}^2 - 2m_u r_b k_2 \mathrm{Sin}(\beta+\theta)\dot{\beta}\dot{\theta} \\
& - m_l r_b k_1 \mathrm{Sin}(\theta)\dot{\theta}^2 - m_u r_b l \mathrm{Sin}(\theta)\dot{\theta}^2 - m_u r_b k_2 \mathrm{Sin}(\beta+\theta)\dot{\theta}^2 \\
& - 2m_w r_b l \mathrm{Sin}(\theta)\dot{\theta}^2 + m_u r_b k_2 \mathrm{Cos}(\beta+\theta)\ddot{\beta} + m_l r_b k_1 \mathrm{Cos}(\theta)\ddot{\theta} \\
& + m_u r_b l \mathrm{Cos}(\theta)\ddot{\theta} + m_u r_b k_2 \mathrm{Cos}(\beta+\theta)\ddot{\theta} + 2m_w r_b l \mathrm{Cos}(\theta)\ddot{\theta} \\
& + i_b\ddot{\phi} + m_b r_b^2\ddot{\phi} + m_l r_b^2\ddot{\phi} + m_u r_b^2\ddot{\phi} + 4m_w r_b^2\ddot{\phi} \\
& + 2m_w r_b r_w \mathrm{Cos}(\gamma)\mathrm{Cos}(\theta)\ddot{\theta} + 2m_w r_b r_w \mathrm{Cos}(\gamma)\mathrm{Cos}(\beta+\theta)\ddot{\theta} \\
& + 2m_w r_b^2 \mathrm{Cos}(\gamma)\mathrm{Cos}(\theta)\ddot{\theta} + 2m_w r_b^2 \mathrm{Cos}(\gamma)\mathrm{Cos}(\beta+\theta)\ddot{\theta} \\
& + 2m_w r_b r_w \mathrm{Cos}(\gamma)\mathrm{Cos}(\beta+\theta)\ddot{\beta} + 2m_w r_b^2 \mathrm{Cos}(\gamma)\mathrm{Cos}(\beta+\theta)\ddot{\beta} \\
& - 2m_w r_b r_w \mathrm{Cos}(\gamma)\mathrm{Sin}(\theta)\dot{\theta}^2 - 2m_w r_b r_w \mathrm{Cos}(\gamma)\mathrm{Sin}(\beta+\theta)\dot{\theta}^2 \\
& - 2m_w r_b^2 \mathrm{Cos}(\gamma)\mathrm{Sin}(\theta)\dot{\theta}^2 - 2m_w r_b^2 \mathrm{Cos}(\gamma)\mathrm{Sin}(\beta+\theta)\dot{\theta}^2 \\
& - 4m_w r_b r_w \mathrm{Cos}(\gamma)\mathrm{Sin}(\beta+\theta)\dot{\beta}\dot{\theta} - 4m_w r_b^2 \mathrm{Cos}(\gamma)\mathrm{Sin}(\beta+\theta)\dot{\beta}\dot{\theta} \\
& - 2m_w r_b^2 \mathrm{Cos}(\gamma)\mathrm{Sin}(\beta+\theta)\dot{\beta}^2 - 2m_w r_b r_w \mathrm{Cos}(\gamma)\mathrm{Sin}(\beta+\theta)\dot{\beta}^2 \\
& + \frac{2i_w r_b^2\ddot{\phi}}{r_w^2} - \frac{2i_w r_b^2\ddot{\theta}}{r_w^2} - \frac{2i_w r_b\ddot{\theta}}{r_w}
\end{aligned} \tag{2}$$

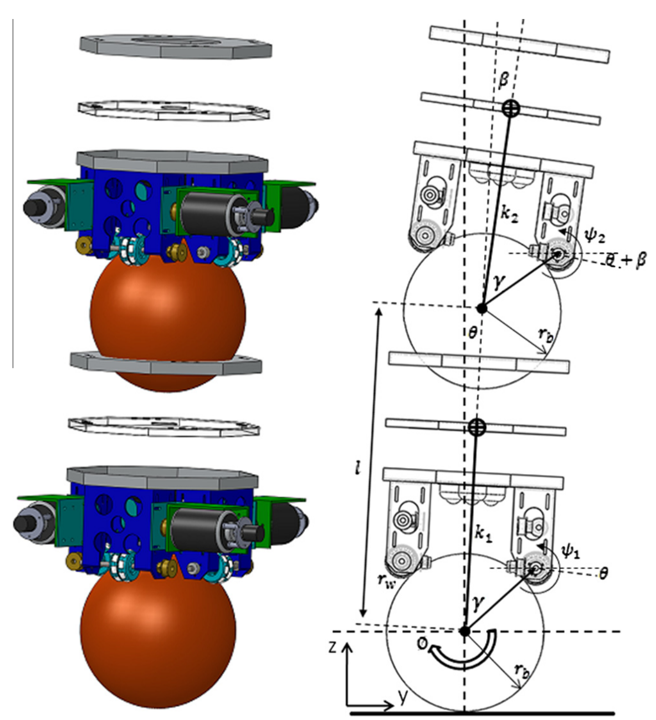

Fig. 3. Double-level ball-riding robot assembly (Left) and projection image of the robot in y–z plane (Right).